

# Discovery and Optimization of Triazolopyrimidinone Derivatives as Selective NLRP3 Inflammasome Inhibitors

David Harrison,\* Mark G. Bock, John R. Doedens, Christopher A. Gabel, M. Katharine Holloway, Arwel Lewis, Jane Scanlon, Andrew Sharpe, Iain D. Simpson, Pamela Smolak, Grant Wishart, and Alan P. Watt



Cite This: *ACS Med. Chem. Lett.* 2022, 13, 1321–1328



Read Online

ACCESS |

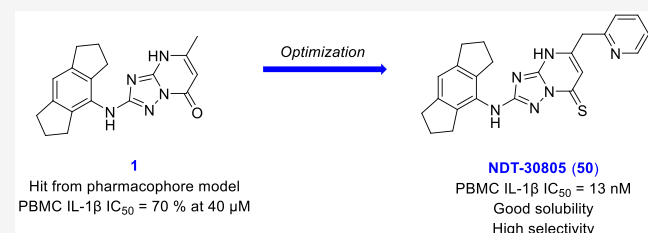
Metrics & More

Article Recommendations

Supporting Information

**ABSTRACT:** The NLRP3 inflammasome is a multiprotein complex that facilitates activation and release of the proinflammatory cytokines interleukin-1 $\beta$  (IL-1 $\beta$ ) and IL-18 in response to infection or endogenous stimuli. It can be inappropriately activated by a range of danger signals resulting in chronic, low-grade inflammation underlying a multitude of diseases, such as Alzheimer's disease, Parkinson's disease, osteoarthritis, and gout. The discovery of potent and specific NLRP3 inhibitors could reduce the burden of several common morbidities. In this study, we identified a weakly potent triazolopyrimidone hit (**1**) following an *in silico* modeling exercise. This was optimized to furnish potent and selective small molecule NLRP3 inflammasome inhibitors. Compounds such as **NDT-30805** could be useful tool molecules for a scaffold-hopping or pharmacophore generation project or used as leads toward the development of clinical candidates.

**KEYWORDS:** NLRP3, inflammasome, interleukin-1, inflammation, innate immunity



**A**n inflammasome is a multiprotein complex of the innate immune system that functions to activate caspase-1 in response to the detection of infection and danger signals.<sup>1</sup> Active caspase-1 catalyzes the conversion of inactive pro-IL-1 $\beta$  and pro-IL-18 into active inflammatory cytokines IL-1 $\beta$  and IL-18. Furthermore, caspase-1 is responsible for the proteolysis and activation of gasdermin D (GSDMD), a process that results in the formation of pores in the cell membrane and a form of lytic cell death known as pyroptosis.

The NLRP3 (NOD-like receptor, Leucine-rich Repeat, and Pyrin-domain-containing protein 3) inflammasome is unique among inflammasomes in that it is assembled in response to a diverse range of endogenous and exogenous danger signals, termed DAMPs (danger-associated molecular patterns) and PAMPs (pathogen-associated molecular patterns). The activation of the NLRP3 inflammasome is a two-step process. The first step (priming) occurs in response to the binding of endogenous cytokines or microbial-derived molecules (e.g., lipopolysaccharide (LPS)) to extracellular receptors such as toll-like receptors (TLRs), IL-1 receptors, and tumor necrosis factor (TNF) receptors.<sup>2</sup> Priming upregulates the transcription and production of NLRP3, pro-IL-1 $\beta$ , and pro-IL-18 through the activation of transcription factor NF- $\kappa$ B. The second step (activation) occurs following the detection of a second stimulus such as a DAMP or PAMP. Activation results in the assembly of the NLRP3 inflammasome and the cleavage of procaspase-1 into the bioactive form of caspase-1, ultimately leading to the release of

proinflammatory cytokines IL-1 $\beta$  and IL-18 into extracellular space.

The discovery of a wide range of danger signals that can activate the NLRP3 inflammasome infers a link to a multitude of human diseases. PAMPs include peptidoglycan and both viral and bacterial DNA and RNA. Some examples of DAMPs are adenosine triphosphate (ATP),<sup>3</sup> amyloid- $\beta$ ,<sup>4</sup> tau,<sup>5,6</sup>  $\alpha$ -synuclein,<sup>7</sup> cholesterol crystals,<sup>8</sup> monosodium urate (MSU) crystals,<sup>9</sup> calcium pyrophosphate crystals,<sup>9</sup> hydroxyapatite,<sup>10</sup> fatty acids,<sup>11</sup> ceramides,<sup>12</sup> asbestos, and silica.<sup>13</sup> Further evidence of the impact of inappropriate NLRP3 activation in humans comes from the study of several gain-of-function mutations causing conditions collectively known as cryopyrin-associated periodic syndromes (CAPS).<sup>14</sup> In these autoinflammatory diseases, the NLRP3 inflammasome exists in an activated state, which leads to dysregulated inflammation. Symptoms vary in severity but may include urticaria on the skin (particularly when exposed to cold), episodic fevers and chills, joint pain or destruction, arthritis, or chronic meningitis leading to neurological damage.

Received: May 20, 2022

Accepted: July 27, 2022

Published: August 1, 2022



ACS Publications

© 2022 American Chemical Society

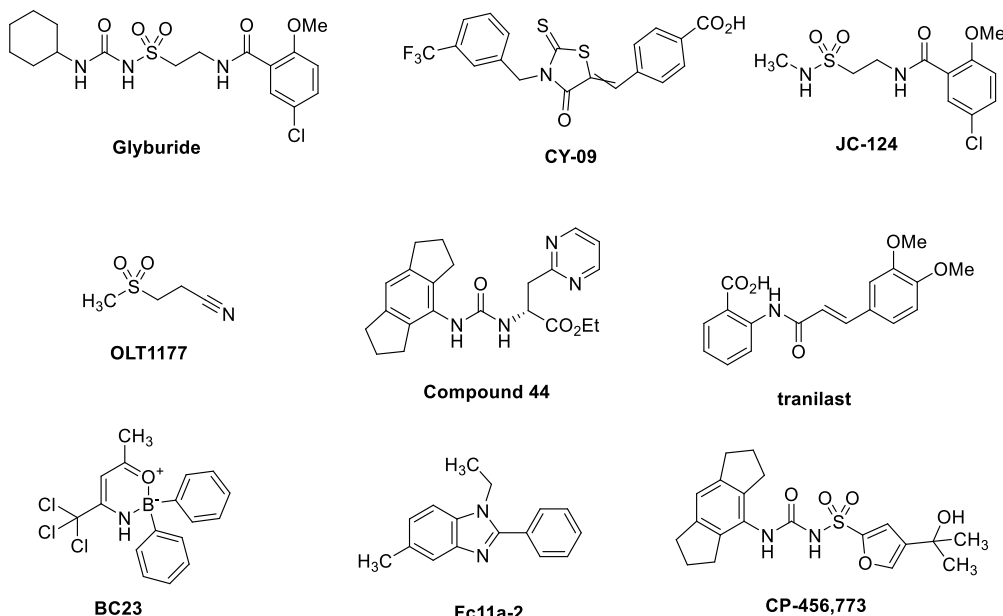


**Figure 1.** Structures of small molecule NLRP3 inflammasome inhibitors.

Many small molecules have been reported to inhibit cytokine release via disruption of the NLRP3 inflammasome pathway, the structures of some of which are shown in Figure 1. Glyburide (glibenclamide) is a widely prescribed sulfonylurea antidiabetic drug, which was shown to inhibit the conversion of pro-IL-1 $\beta$  into its active form.<sup>15</sup> Further studies revealed that glyburide disrupted the formation of the NLRP3 inflammasome.<sup>16</sup> CY-09, a rhodanine-based molecule, blocks NLRP3 inflammasome activation by directly binding to the NLRP3 NACHT domain.<sup>17</sup> A molecule with some identical structural features to glyburide, JC-124, was identified as an NLRP3 inhibitor, which showed an effect in a mouse model of Alzheimer's disease.<sup>18,19</sup> OLT-1177 (dapansutript) is a low-molecular-weight  $\beta$ -sulfonylnitrile compound that has been tested in a phase IIa clinical trial for acute gout flares.<sup>20</sup> It is reported to be a selective NLRP3 inhibitor and exhibited an anti-inflammatory effect in mouse *in vivo* studies.<sup>21</sup> Ester 44 was recently disclosed among a series of selective NLRP3 inflammasome inhibitors, displaying excellent potency in a whole blood assay and high permeability.<sup>22</sup> Other molecules with reported inhibition of the NLRP3 inflammasome include the natural product tranilast,<sup>23</sup> the oxazaborine complex BC23,<sup>24</sup> and the benzimidazole Fc11a-2.<sup>25</sup> Several reviews have been published detailing these and further NLRP3 inflammasome-disrupting molecules.<sup>26–32</sup>

The most widely studied NLRP3 inhibitor is CP-456,773 (CRID3/MCC950). It was designed to be an IL-1 $\beta$  inhibitor in the late 1990s, prior to the discovery of the inflammasome, using glyburide as the starting point.<sup>33</sup> Subsequent studies by Coll and co-workers showed this to be a specific NLRP3 inhibitor.<sup>34</sup> Recently, two groups have published crystal structures illustrating that CP-456,773 and related sulfonylurea inhibitor NP3-146 bind close to the NACHT domain of the NLRP3 complex, stabilizing its inactive conformation.<sup>35,36</sup>

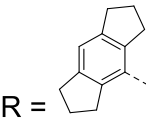
CP-456,773 has been tested in numerous *in vitro* and *in vivo* models that have revealed disease-relevant effects in multiple conditions such as Alzheimer's disease,<sup>37</sup> Parkinson's disease,<sup>38</sup> chronic kidney disease,<sup>39</sup> gout,<sup>34</sup> inflammatory bowel disease,<sup>40</sup> rheumatoid arthritis,<sup>41</sup> and asthma.<sup>42</sup> These discoveries serve to validate NLRP3 inflammasome inhibition as a promising strategy

for the treatment of wide-ranging diseases related to inflammation.

Although several clinical trials for small molecule inhibitors of the NLRP3 inflammasome have been reported, none have reached market approval. Since the MCC950 disclosure by Coll and co-workers, there has been great interest in the search for novel NLRP3 inflammasome inhibitors. Several drug discovery programs have used CP-456,773 as the chemical starting point, yet owing to the acidic center and high polar surface area, the physicochemical properties of this molecule and related sulfonylureas (such as the acidic center and high polar surface area) are suboptimal for facile membrane permeability and CNS penetration. Accordingly, there remains a need for selective NLRP3 inflammasome inhibitors that are structurally distinct from the sulfonylureas, as these could possess different properties and therefore have potentially different applications. Furthermore, the discovery of more diverse compounds could contribute to a greater understanding of the pharmacophoric requirements for NLRP3 inflammasome inhibitors.

We began our search for novel NLRP3 inflammasome inhibitors by building a pharmacophore model based on proprietary molecules. We used a range of structurally diverse, selective NLRP3 inflammasome inhibitors and refined the model with data from our in-house "active" and "inactive" molecules to improve the outcome. An *in silico* screening of various molecules identified a low-molecular-weight (321 Da) triazolopyrimidinone hit (**1**). This was screened in our primary assay, a peripheral blood mononuclear cell (PBMC) assay that measured IL-1 $\beta$  release following stimulation with lipopolysaccharide (LPS) and adenosine triphosphate (ATP) and showed a consistent inhibition of IL-1 $\beta$  release of 70% at 40  $\mu$ M. Following the discovery of this weak hit, a structure–activity relationship investigation was undertaken to improve upon the potency of **1**, the results of which are shown in Table 1.

Initially, some fundamental changes to the bicyclic core were explored. Methylation of the 4-nitrogen (**2**) and removal of the carbonyl (**3**) resulted in a complete loss of inhibition (defined as having an IC<sub>50</sub> greater than 40  $\mu$ M in the PBMC assay), as did the change to a structurally isomeric triazolopyrimidinone core (**4**).

**Table 1.** Initial Screening Hit and SAR


Compound	Structure	PBMC IC <sub>50</sub>
1		70 ± 22 % at 40 μM (n=3)
2		>40 μM (n=2)
3		>40 μM (n=2)
4		>40 μM (n=3)
5		57 ± 26 % at 40 μM (n=5)
6		>40 μM (n=2)
7		>40 μM (n=2)
8		>40 μM (n=2)
9		>40 μM (n=2)
10		>40 μM (n=2)

Replacement of the 3-nitrogen with carbon to give **5** resulted in a small reduction in activity. We chose to retain the 4*H*,7*H*-[1,2,4]triazolo[1,5-*a*]pyrimidin-7-one core and probed the SAR by introducing various substituents. At the 6-position, the addition of a methyl group either with the 5-methyl removed (**6**), or retained (**7**), ablated activity. Similarly, substitution with 6-benzyl (**8**), 6-methoxy (**9**), or 6-cyano (**10**) gave inactive compounds.

Next, we turned our attention to the 5-position. Primary assay data for the synthesized compounds are shown in **Table 2**. Replacement of the 5-methyl with hydrogen (**11**) had little effect on IL-1 $\beta$  inhibition. Exchange of the methyl for various larger substituents including ethyl (**12**), methoxyethyl (**13**), benzyl (**14**), phenethyl (**15**) and 4-tetrahydropyranyl (**16**) all resulted in compounds with single-digit micromolar IC<sub>50</sub> values. The tolerance for basic groups in the 5-position was less encouraging, with 4-piperidinyl (**17**), 1-methyl-4-piperidinyl (**18**), and 3-piperidinyl (**19**) analogues not inhibiting at the top concentration, although 5-(1-methyl-3-piperidine) substitution (**20**) did result in an improvement in potency compared to compound **1**. Of the compounds profiled thus far, **14** displayed the best potency. Encouraged by this, a more focused set of analogues

containing a methylene-spaced cyclic group in the 5-position (**21** to **48**) were investigated. The cyclohexyl analogue **21** was slightly less potent than the benzyl equivalent, and a range of benzyl analogues scanning *ortho*-, *meta*-, and *para*-substitution (**22** to **30**) did not identify any compounds more potent than the unsubstituted matched pair. A scan of methylene-linked pyridyl analogues (**31** (NDT-30347) to **33**) led to a further boost in potency; the 2-pyridyl group was shown to be favored over the other two isomers, with PBMC activity an order of magnitude greater than that of the benzyl **14**. The 2-pyrimidinyl **34** was synthesized as a close analogue of the potent 2-pyridyl lead, but the additional nitrogen was detrimental to potency. Profiling of analogues bearing both basic and nonbasic saturated heterocycles (**35** to **43**) brought mixed results. No potency improvements over benzyl **14** were made, yet the equipotent 2-tetrahydropyranyl compound, **36** (NDT-30408), offered potential advantages owing to its greater sp<sup>3</sup> character, lower lipophilicity, and reduced aromatic ring count. These parameters are commonly associated with improved developability characteristics such as solubility. Finally, an investigation of azoles (**44** to **48**) revealed that the 1-methyl-3-pyrazolyl was equipotent to benzyl **14**, but no superior compounds were identified.

In addition to the extensive SAR investigation into the 5-position, we returned to hit **1** and synthesized the corresponding thiocarbonyl analogue **49**. To our surprise, this single atom change greatly increased the potency. Gratifyingly, applying this switch from carbonyl to thiocarbonyl on two additional molecules (**31** and **36**, resulting in **50** (NDT-30805) and **51** (NDT-30744), respectively) had a similar potency boosting effect. Both thiocarbonyl molecules were an order of magnitude more potent than the carbonyl matched pairs in the PBMC assay.

With a structure–activity relationship now established and several molecules identified as interesting leads, we selected the two most potent thiocarbonyl compounds **50** (NDT-30805) and **51** (NDT-30744) for further profiling, along with the corresponding carbonyl matched pairs **31** (NDT-30347) and **36** (NDT-30408). The synthetic route to **31**, **36**, **50**, and **51** is shown in **Scheme 1**. The aminotriazole ring was formed in two steps starting from the corresponding aniline. Reaction with dimethyl cyanocarbonimidodithioate gave the thiourea derivative, which was subsequently cyclized with hydrazine hydrate. The aminotriazole was condensed with a  $\beta$ -keto ester by refluxing in acetic acid to give the triazolopyrimidone compounds **31** and **36**. The corresponding thiocarbonyl derivatives were then prepared using phosphorus pentasulfide.

Some calculated properties and additional *in vitro* data for the four lead molecules are shown in **Table 3**. All four molecules are classified as lipophilic, with log P values at the upper end or above the desirable range for orally bioavailable drugs. The lipophilic character of the compounds contributes to very high protein binding, with free fractions in human plasma for **31**, **36**, and **51** at or below 0.2%. Compound **50** has the largest free fraction, which is 1.9% in human plasma. The thermodynamic solubility varies; the carbonyl compounds **31** and **36** have low aqueous solubility, while the corresponding thiocarbonyls **50** and **51** possess high solubility. Compounds **31**, **50**, and **51** have very low membrane permeability, and **36** has a permeability of 0.38 nm/s, as measured in a PAMPA assay.

In addition to the cellular potency assay, the activity of each lead compound was measured in human whole blood (WB), following a similar protocol to the PBMC assay. The IC<sub>50</sub> of a compound in this assay is affected by protein binding. The highly bound nature of **31**, **36**, **50**, and **51** results in a large attenuation

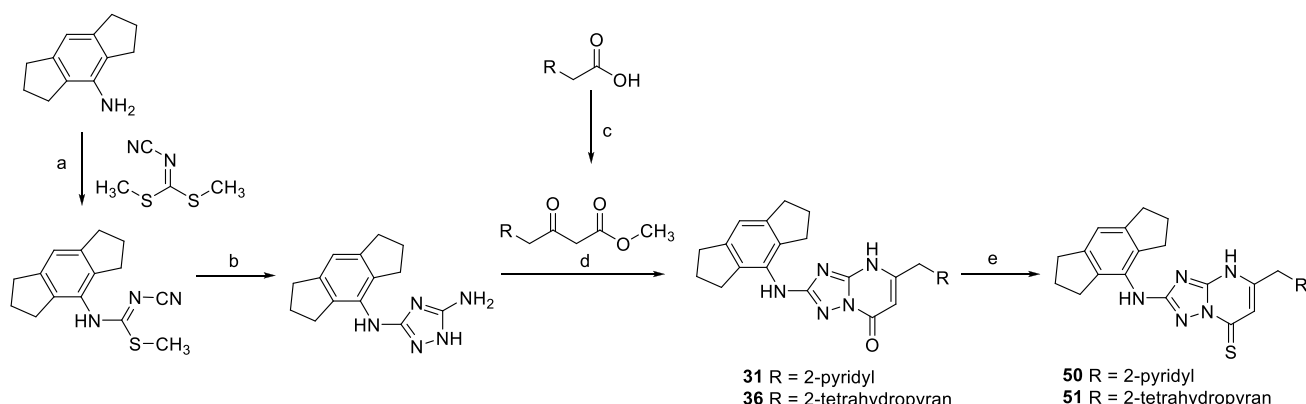
Table 2. 5-Position Modifications and SAR

Compound	X	PBMC IC <sub>50</sub>	IL-1β
11	H	77 ± 18 % at 40 μM (n=3)	
12	Ethyl	8.7 (n=2), range 8.4 – 9.1	
13	<chem>CCCOc1ccccc1</chem>	2.8 (n=2), range 1.2 – 4.5	
14	Benzyl	1.8 ± 0.50 (n=4)	
15	<chem>CCc1ccccc1</chem>	3.4 (n=2), range 2.5 – 4.3	
16	<chem>CC1CCOC1</chem>	6.3 (n=1)	
17	<chem>CC1CCNCC1</chem>	>40 (n=1)	
18	<chem>CC1CCN(C)CC1</chem>	>40 (n=3)	
19	<chem>CC1CCNCC1</chem>	>40 (n=2)	
20	<chem>CC1CCN(C)CC1</chem>	4.9 ± 2.9 (n=4)	
21	<chem>CC1CCCCC1</chem>	4.5 ± 2.6 (n=4)	
22	<chem>CC1=CC=C(O)c2ccccc21</chem>	3.0 (n=2), range 0.97 – 5.1	
23	<chem>CC1=CC=C(Cl)c2ccccc21</chem>	ND (solubility)	
24	<chem>CC1=CC=C(Cl)c2ccccc21</chem>	2.8 ± 2.7 (n=3)	
25	<chem>CC1=CC=C(Cl)c2ccccc21</chem>	10 (n=1)	
26	<chem>CC1=CC=C#Nc2ccccc21</chem>	ND (solubility)	
27	<chem>CC1=CC=C#Nc2ccccc21</chem>	2.4 (n=1)	
28	<chem>CC1=CC=C#Nc2ccccc21</chem>	1.6 ± 0.52 (n=3)	
29	<chem>CC1=CC=C#Nc2ccccc21</chem>	4.0 (n=1)	
30	<chem>CC1=CC=C#Nc2ccccc21</chem>	3.7 (n=2), range 2.3 – 5.0	
31 (NDT-30347)	<chem>CC1=CC=C#Nc2ccccc21</chem>	0.26 (n=2), range 0.22 – 0.31	
32	<chem>CC1=CC=C#Nc2ccccc21</chem>	3.4 ± 2.3 (n=3)	
33	<chem>CC1=CC=C#Nc2ccccc21</chem>	5.8 (n=2), range 2.8 – 8.8	
34	<chem>CC1=CC=C#Nc2ccccc21</chem>	1.7 ± 0.97 (n=6)	
35	<chem>CC1=CC=C#Nc2ccccc21</chem>	5.0 (n=1)	
36 (NDT-30408)	<chem>CC1=CC=C#Nc2ccccc21</chem>	1.9 ± 1.1 (n=5)	
37	<chem>CC1=CC=C#Nc2ccccc21</chem>	3.4 ± 1.9 (n=3)	
38	<chem>CC1=CC=C#Nc2ccccc21</chem>	7.8 ± 3.8 (n=3)	
39	<chem>CC1=CC=C#Nc2ccccc21</chem>	20 (n=2), range 14 – 25	
40	<chem>CC1=CC=C#Nc2ccccc21</chem>	8.8 (n=2), range 4.7 – 13	
41	<chem>CC1=CC=C#Nc2ccccc21</chem>	5.4 (n=2), range 2.4 – 8.3	
42	<chem>CC1=CC=C#Nc2ccccc21</chem>	6.0 ± 2.2 (n=3)	
43	<chem>CC1=CC=C#Nc2ccccc21</chem>	>40 (n=2)	
44	<chem>CC1=CC=C#Nc2ccccc21</chem>	2.0 ± 1.1 (n=4)	
45	<chem>CC1=CC=C#Nc2ccccc21</chem>	1.8 ± 1.1 (n=4)	
46	<chem>CC1=CC=C#Nc2ccccc21</chem>	4.9 (n=1)	
47	<chem>CC1=CC=C#Nc2ccccc21</chem>	5.5 ± 1.8 (n=3)	
48	<chem>CC1=CC=C#Nc2ccccc21</chem>	16 (n=1)	
49	<chem>CC1=CC=C#Nc2ccccc21</chem>	0.60 ± 0.34 (n=5)	
50 (NDT-30805)	<chem>CC1=CC=C#Nc2ccccc21</chem>	0.013 ± 0.0007 (n=3)	
51 (NDT-30744)	<chem>CC1=CC=C#Nc2ccccc21</chem>	0.13 ± 0.13 (n=4)	

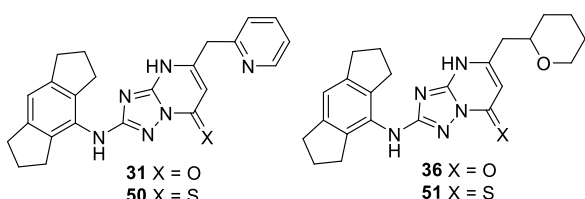
between PBMC and WB potency. NDT-30805 (**50**) is the most active compound from this series and is approximately 2-fold more potent than the widely studied NLRP3 inflammasome

inhibitor CP-456,773 in both PBMC and whole blood assays (reported IC<sub>50</sub> = 0.030 and 2.9 μM, respectively).<sup>22</sup>

The genesis of the above four compounds is from the original triazolopyrimidone hit (**1**), itself derived from our pharmaco-

**Scheme 1. Synthesis of Compounds 31, 36, 50, and 51<sup>a</sup>**

<sup>a</sup>Reagents and conditions: (a) NaH, DMF, 70 °C; (b) hydrazine hydrate, EtOH, 110 °C; (c) potassium 3-methoxy-3-oxopropanoate, CDI, MgCl<sub>2</sub>, MeCN, 0 °C; (d) AcOH, 110 °C; (e) phosphorus pentasulfide, dioxane, 70 °C.

**Table 3. Profiling of Lead Molecules**

compound	31 (NDT-30347)	36 (NDT-30408)	50 (NDT-30805)	51 (NDT-30744)
MW	398	405	414	421
c log P (ChemAxon)	4.8	4.4	5.1	5.2
tPSA	85	78	68	64
PAMPA, nm/s	<0.18	0.38	<0.18	<0.004
thermodynamic solubility, mg/mL [μM]	0.0009 [2.4]	0.0097 [24]	0.61 [1500]	0.31 [730]
PPB, %	Hu = 99.8 Rat = 100	Hu = 99.9 Rat = 100	Hu = 98.1 Rat = 98.5	Hu = 99.9 Rat = 99.8
PBMC IL-1β IC <sub>50</sub> , μM	0.26 (n = 2), range 0.22–0.31	1.9 ± 1.1 (n = 5)	0.013 ± 0.0007 (n = 3)	0.13 ± 0.13 (n = 4)
WB IL-1β IC <sub>50</sub> , μM	>40 (n = 2)	>40 (n = 1)	1.5 ± 0.63 (n = 3)	8.9 ± 7.6 (n = 4)
ASC speck inh IC <sub>50</sub> , μM	0.24 (n = 1)	1.3 (n = 1)	0.034 (n = 1)	0.19 (n = 1)
PBMC IL-6 IC <sub>50</sub> , μM	>40 (n = 1)	>40 (n = 1)	>40 (n = 1)	>20 (n = 1)
PBMC TNFα IC <sub>50</sub> , μM	>40 (n = 1)	>40 (n = 1)	>40 (n = 1)	>20 (n = 1)

phore model. Figure 2 shows compound **50** docked into the NLRP3 NACHT domain of the recently disclosed cocrystal structure of the sulfonylurea NP3–146.<sup>30</sup> The hexahydroindacene moiety is buried in a lipophilic pocket coplanar with the aromatic ring of NP3–146, with the anilinic NH also overlaid. The 2-nitrogen of the triazolo ring may act as an H-bond acceptor of Ala228; the thiocarbonyl is in the H-bonding range of several residues as illustrated in the ligand interaction plot (Figure 2b). The methylene-spaced 2-pyridyl substituent occupies similar space to the tertiary alcohol of NP3–146 but projects further out of the binding pocket and into solvent space. The favorable docking pose of **50**, which fits well into the ligand binding pocket occupied by NP3–146, affords a rationale for the good cellular potency.

Further mechanistic evidence of selective NLRP3 inflammasome inhibition was obtained from an ASC speck assay and IL-6/TNFα selectivity assays. The ASC speck assay uses green fluorescent protein (GFP)-tagged ASC, a component of the NLRP3 inflammasome. The activation of the inflammasome with LPS and nigericin results in fluorescence, the disruption of

which is measured by confocal microscopy. The selectivity assays look at downstream cytokines IL-6 and TNFα, neither of which should be affected by a selective inhibitor during the time frame of the assay. All four molecules **31**, **36**, **50**, and **51** show a mechanistic profile consistent with a selective disruptor of NLRP3 inflammasome formation, as evidenced by the inhibition of ASC speck formation and lack of effect on inflammatory cytokines IL-6 and TNFα.

In summary, an *in silico* pharmacophore model was generated by overlaying several structurally diverse NLRP3 inflammasome inhibitors and subsequent refinement with proprietary screening data. Using this model, we were able to discover a weakly potent triazolopyrimidine hit, **1**. Subsequent optimization led to the identification of a novel chemotype of NLRP3 inflammasome inhibitors, as exemplified by **NDT-30805** (**50**). This is a potent, selective, and highly soluble molecule. Its advantages over CP-456,773 are superior potency and that it is uncharged at physiological pH (compared with the acidic characteristic of the sulfonylurea). Its disadvantages are high protein binding and low permeability, which in part may derive from the high lipophilicity

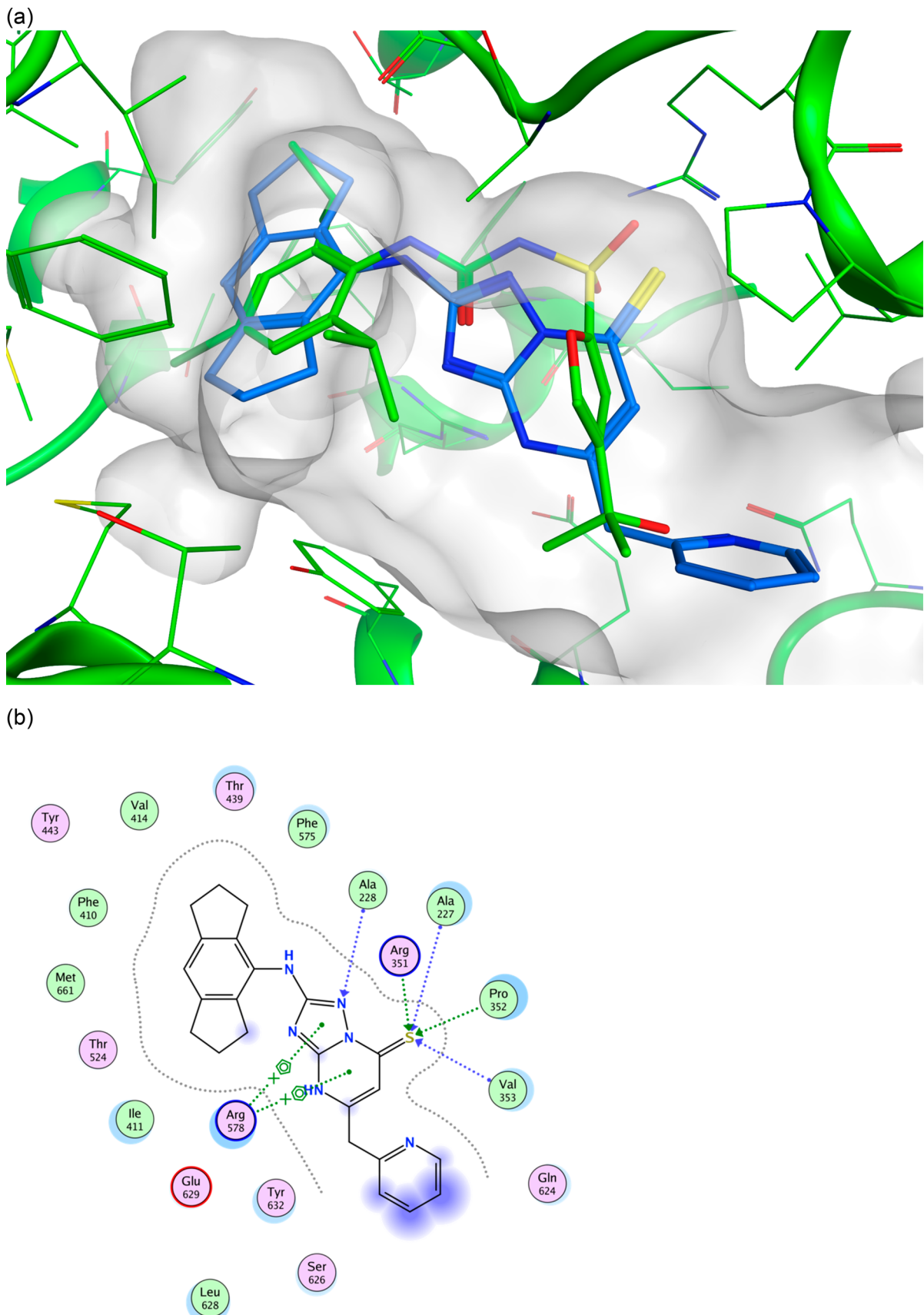


**Figure 2.** (a) Docked pose of one tautomer of NDT-30805 (**50**) shown in blue in the NLRP3 NACHT domain structure 7ALV binding site. The 7ALV ligand NP3-146 is shown in green for comparison. (b) Ligand interaction plot of the docked pose of NDT-30805 (**50**).

( $c \log P = 5.1$ ) and aromatic character (four aromatic rings,  $\text{fsp}^3 = 0.30$ ). The SAR around the hexahydroindacene moiety was not explored during this work, so this would be a potentially fruitful area for future exploration. The molecules described in this study could further refine the NLRP3 inflammasome inhibitor pharmacophore and provide potential starting points for further optimization toward the discovery of clinical candidates for the treatment of inflammatory diseases.

## ■ ASSOCIATED CONTENT

### § Supporting Information

The Supporting Information is available free of charge at <https://pubs.acs.org/doi/10.1021/acsmmedchemlett.2c00242>.

Assay protocols for PBMC IL-1 $\beta$ , whole blood IL-1 $\beta$ , PBMC IL-6, PBMC TNF $\alpha$ , ASC-speck, PAMPA, and thermodynamic solubility assays, details of docking studies, and synthesis and spectral data for compounds 1 to 51 ([PDF](#))

## ■ AUTHOR INFORMATION

### Corresponding Author

David Harrison – NodThera Ltd., Saffron Walden, Essex CB10 1XL, United Kingdom;  [orcid.org/0000-0001-6258-3254](https://orcid.org/0000-0001-6258-3254); Email: [david.harrison@nodthera.com](mailto:david.harrison@nodthera.com)

### Authors

Mark G. Bock – NodThera Inc., Lexington, Massachusetts 02420, United States

John R. Doedens – NodThera Inc., Seattle, Washington 98103, United States

Christopher A. Gabel – NodThera Inc., Seattle, Washington 98103, United States

M. Katharine Holloway – Gfree Bio LLC, Austin, Texas 78730, United States;  [orcid.org/0000-0002-0849-2658](https://orcid.org/0000-0002-0849-2658)

Arwel Lewis – Charles River Laboratories, Saffron Walden, Essex CB10 1XL, United Kingdom

Jane Scanlon – NodThera Ltd., Saffron Walden, Essex CB10 1XL, United Kingdom

Andrew Sharpe – Charles River Laboratories, Saffron Walden, Essex CB10 1XL, United Kingdom

Iain D. Simpson – Charles River Laboratories, Saffron Walden, Essex CB10 1XL, United Kingdom

Pamela Smolak – NodThera Inc., Seattle, Washington 98103, United States

Grant Wishart – Charles River Laboratories, Saffron Walden, Essex CB10 1XL, United Kingdom

Alan P. Watt – NodThera Ltd., Saffron Walden, Essex CB10 1XL, United Kingdom

Complete contact information is available at:

<https://pubs.acs.org/10.1021/acsmmedchemlett.2c00242>

### Funding

The work contained within this manuscript was funded entirely by NodThera, Inc.

### Notes

The authors declare no competing financial interest.

## ■ ACKNOWLEDGMENTS

The authors would like to thank Matthew Boyton, Enrique Garcia-Alvarez, and their colleagues at Charles River Discovery Services in Portishead, UK, for generating much of the screening data. We also acknowledge the role of Han Xuejun and co-

workers at WuXi AppTec in Tianjin, China, for the synthesis and analysis of many compounds. We thank Adam Keeney, President of NodThera Inc., for supporting the research that led to this manuscript.

## ■ ABBREVIATIONS

NLRP3, NOD-like receptor, Leucine-rich Repeat, and Pyrin-domain-containing protein 3; PAMP, pathogen-associated molecular pattern; DAMP, danger-associated molecular pattern; PBMC, peripheral blood mononuclear cell; ASC, apoptosis-associated speck-like protein containing a CARD

## ■ REFERENCES

- Martinon, F.; Burns, K.; Tschoopp, J. The inflammasome: a molecular platform triggering activation of inflammatory caspases and processing of pro IL-1 $\beta$ . *Mol. Cell* **2002**, *10* (2), 417–426.
- He, Y.; Hara, H.; Nuñez, G. Mechanism and regulation of NLRP3 inflammasome activation. *Trends Biochem. Sci.* **2016**, *41*, 1012–1021.
- Mariathasan, S.; Weiss, D. S.; Newton, K.; McBride, J.; O'Rourke, K.; Roose-Girma, M.; Lee, W. P.; Weinrauch, Y.; Monack, D. M.; Dixit, V. M. Cryopyrin activates the inflammasome in response to toxins and ATP. *Nature* **2006**, *440* (7081), 228–232.
- Halle, A.; Hornung, V.; Petzold, G. C.; Stewart, C. R.; Monks, B. G.; Reinheckel, T.; Fitzgerald, K. A.; Latz, E.; Moore, K. J.; Golenbock, D. T. The NALP3 inflammasome is involved in the innate immune response to amyloid-beta. *Nat. Immunol.* **2008**, *9* (8), 857–865.
- Stancu, I.-C.; Cremers, N.; Vanrusselt, H.; Couturier, J.; Vanoostruylse, A.; Kessels, S.; Lodder, C.; Brône, B.; Huaux, F.; Octave, J.-N.; Terwel, D.; Dewachter, I. Aggregated Tau activates NLRP3-ASC inflammasome exacerbating exogenously seeded and non-exogenously seeded Tau pathology in vivo. *Acta Neuropath.* **2019**, *137*, 599–617.
- Ising, C.; Venegas, C.; Zhang, S.; Scheiblich, H.; Schmidt, S. V.; Vieira-Saecker, A.; Schwartz, S.; Albasset, S.; McManus, R. M.; Tejera, D.; Griep, A.; Santarelli, F.; Brosseron, F.; Opitz, S.; Stunder, J.; Merten, M.; Kayed, R.; Golenbock, D. T.; Blum, D.; Latz, E.; Buée, L.; Heneka, M. T. NLRP3 inflammasome activation drives tau pathology. *Nature* **2019**, *575*, 669–673.
- Codolo, G.; Plotegher, N.; Pozzobon, T.; Brucale, M.; Tessari, I.; Bubacco, L.; de Bernard, M. Triggering of Inflammasome by Aggregated  $\alpha$ -Synuclein, an Inflammatory Response in Synucleinopathies. *PLOS One* **2013**, *8* (1), e55375.
- Duewell, P.; Kono, H.; Rayner, K. J.; Sirois, C. M.; Vladimer, G.; Bauernfeind, F. G.; Abela, G. S.; Franchi, L.; Núñez, G.; Schnurr, M.; Espenik, T.; Lien, E.; Fitzgerald, K. A.; Rock, K. L.; Moore, K. J.; Wright, S. D.; Hornung, V.; Latz, E. NLRP3 inflammasomes are required for atherosclerosis and activated by cholesterol crystals. *Nature* **2010**, *464*, 1357–1361.
- Martinon, F.; Pétrilli, V.; Mayor, A.; Tardivel, A.; Tschoopp, J. Gout-associated uric acid crystals activate the NALP3 inflammasome. *Nature* **2006**, *440*, 237–241.
- Jin, C.; Frayssinet, P.; Pelker, R.; Cwirka, D.; Hu, B.; Vignery, A.; Eisenbarth, S. C.; Flavell, R. A. NLRP3 inflammasome plays a critical role in the pathogenesis of hydroxyapatite-associated arthropathy. *Proc. Natl. Acad. Sci. U.S.A.* **2011**, *108* (36), 14867–14872.
- Wen, H.; Gris, D.; Lei, Y.; Jha, S.; Zhang, L.; Huang, M. T.-H.; Brickey, W. J.; Ting, J. P.-Y. Fatty acid-induced NLRP3-ASC inflammasome activation interferes with insulin signaling. *Nat. Immunol.* **2011**, *12*, 408–415.
- Scheiblich, H.; Schlüter, A.; Golenbock, D. T.; Latz, E.; Martinez-Martinez, P.; Heneka, M. T. Activation of the NLRP3 inflammasome in microglia: the role of ceramide. *J. Neurochem.* **2017**, *143*, 534–550.
- Dostert, C.; Pétrilli, V.; Van Bruggen, R.; Steele, C.; Mossman, B. T.; Tschoopp, J. Innate immune activation through Nalp3 inflammasome sensing of asbestos and silica. *Science* **2008**, *320* (5876), 674–677.
- Hoffman, H. M.; Mueller, J. L.; Broide, D. H.; Wanderer, A. A.; Kolodner, R. D. Mutation of a new gene encoding a putative pyrin-like

- protein causes familial cold autoinflammatory syndrome and Muckle-Wells syndrome. *Nat. Genet.* **2001**, *29* (3), 301–305.
- (15) Perregaux, D. G.; McNiff, P.; Laliberte, R.; Hawryluk, N.; Peurano, H.; Stam, E.; Eggler, J.; Griffiths, R.; Dombroski, M. A.; Gabel, A. A. Identification and characterization of a novel class of interleukin-1 post-translational processing inhibitors. *J. Pharmacol. Exp. Ther.* **2001**, *299* (1), 187–197.
- (16) Lamkanfi, M.; Mueller, J. L.; Vitari, A. C.; Misaghi, S.; Fedorova, A.; Deshayes, K.; Lee, W. P.; Hoffman, H. M.; Dixit, V. M. Glyburide inhibits the Cryopyrin/Nalp3 inflammasome. *J. Cell. Biol.* **2009**, *187* (1), 61–70.
- (17) Jiang, H.; He, H.; Chen, Y.; Huang, W.; Cheng, J.; Ye, J.; Wang, A.; Tao, J.; Wang, C.; Liu, Q.; Jin, T.; Jiang, W.; Deng, X.; Zhou, R. Identification of a selective and direct NLRP3 inhibitor to treat inflammatory disorders. *J. Exp. Med.* **2017**, *214* (11), 3219–3238.
- (18) Yin, J.; Zhao, F.; Chojnacki, J. E.; Fulp, J.; Klein, W. L.; Zhang, S.; Zhu, X. NLRP3 Inflammasome Inhibitor Ameliorates Amyloid Pathology in a Mouse Model of Alzheimer's Disease. *Mol. Neurobiol.* **2018**, *55* (3), 1977–1987.
- (19) Fulp, J.; He, L.; Toldo, S.; Jiang, Y.; Boice, A.; Guo, C.; Li, X.; Rolfe, A.; Sun, D.; Abbate, A.; Wang, X.-Y.; Zhang, S. Structural Insights of Benzenesulfonamide Analogues as NLRP3 Inflammasome Inhibitors: Design, Synthesis, and Biological Characterization. *J. Med. Chem.* **2018**, *61* (12), 5412–5423.
- (20) Klück, V.; Jansen, T. L. A.; Janssen, M.; Comarniceanu, A.; Efdé, M.; Tengesdal, I. W.; Schraa, K.; Cleophas, M. C. P.; Scribner, C. L.; Skouras, D. B.; Marchetti, C.; Dinarello, C. A.; Joosten, L. A. B. Dapansutript, an oral selective NLRP3 inflammasome inhibitor, for treatment of gout flares: an open-label, dose-adaptive, proof-of-concept, phase 2a trial. *Lancet Rheumatol.* **2020**, *2* (5), e270–e280.
- (21) Marchetti, C.; Swartzwelter, B.; Gamboni, F.; Neff, C. P.; Richter, K.; Azam, T.; Carta, S.; Tengesdal, I.; Nemkov, T.; D'Alessandro, A.; Henry, C.; Jones, G. S.; Goodrich, S. A.; St. Laurent, J. P.; Jones, T. M.; Scribner, C. L.; Barrow, R. B.; Altman, R. D.; Skouras, D. B.; Gattorno, M.; Grau, V.; Janciauskiene, S.; Rubartelli, A.; Joosten, L. A. B.; Dinarello, C. A. OLT1177, a  $\beta$ -sulfonyl nitrile compound, safe in humans, inhibits the NLRP3 inflammasome and reverses the metabolic cost of inflammation. *Proc. Natl. Acad. Sci. U.S.A.* **2018**, *115* (7), e1530–e1539.
- (22) Harrison, D.; Boutard, N.; Brzozka, K.; Bugaj, M.; Chmielewski, S.; Cierpich, A.; Doedens, J. R.; Fabritius, C.-H. R. Y.; Gabel, C. A.; Galeowski, M.; Kowalczyk, P.; Levenets, O.; Mroczkowska, M.; Palica, K.; Porter, R. A.; Schultz, D.; Sowinska, M.; Topolnicki, G.; Urbanski, P.; Woyciechowski, J.; Watt, A. P. Discovery of a series of ester-substituted NLRP3 inflammasome inhibitors. *Bioorg. Med. Chem. Lett.* **2020**, *30* (23), 127560.
- (23) Huang, Y.; Jiang, H.; Chen, Y.; Wang, X.; Yang, Y.; Tao, J.; Deng, X.; Liang, G.; Zhang, H.; Jiang, W.; Zhou, R. Tranilast directly targets NLRP3 to treat inflammasome-driven diseases. *EMBO Mol. Med.* **2018**, *10* (4), e8689.
- (24) Baldwin, A. G.; Rivers-Auty, J.; Daniels, M. J. D.; White, C. S.; Schwalbe, C. H.; Schilling, T.; Hammadi, H.; Jaiyong, P.; Spencer, N. G.; England, H.; Luheshi, N. M.; Kadirvel, M.; Lawrence, C. B.; Rothwell, N. J.; Harte, M. K.; Bryce, R. A.; Allan, S. M.; Eder, C.; Freeman, S.; Brough, D. Boron-based inhibitors of the NLRP3 inflammasome. *Cell Chem. Biol.* **2017**, *24* (11), 1321–1335.
- (25) Liu, W.; Guo, W.; Wu, J.; Luo, Q.; Tao, F.; Gu, Y.; Shen, Y.; Li, J.; Tan, R.; Xu, Q.; Sun, Y. A novel benzo[d]imidazole derivate prevents the development of dextran sulfate sodium-induced murine experimental colitis via inhibition of NLRP3 inflammasome. *Biochem. Pharmacol.* **2013**, *85* (10), 1504–1512.
- (26) El-Sharkawy, L.; Brough, D.; Freeman, S. Inhibiting the NLRP3 Inflammasome. *Molecules* **2020**, *25* (23), 5533.
- (27) Mangan, M. S. J.; Olhava, E. J.; Roush, W. R.; Seidel, H. M.; Glick, G. D.; Latz, E. Targeting the NLRP3 inflammasome in inflammatory diseases. *Nat. Rev. Drug Discovery* **2018**, *17*, 588–606.
- (28) Zahid, A.; Li, B.; Kombe Kombe, A. J.; Jin, T.; Tao, J. Pharmacological Inhibitors of the NLRP3 Inflammasome. *Front. Immunol.* **2019**, *10*, 2538.
- (29) Zhang, X.; Xu, A.; Lv, J.; Zhang, Q.; Ran, Y.; Wei, C.; Wu, J. Development of small molecule inhibitors targeting NLRP3 inflammasome pathway for inflammatory diseases. *Eur. J. Med. Chem.* **2020**, *185*, 111822.
- (30) Schwaid, A. G.; Spencer, K. B. Strategies for Targeting the NLRP3 Inflammasome in the Clinical and Preclinical Space. *J. Med. Chem.* **2021**, *64* (1), 101–122.
- (31) Platnick, J. M.; Muruve, D. A. NOD-like receptors and inflammasomes: A review of their canonical and non-canonical signaling pathways. *Arch. Biochem. Biophys.* **2019**, *670*, 4–14.
- (32) Coll, R. C.; Schroder, K.; Pelegrin, P. NLRP3 and pyroptosis blockers for treating inflammatory diseases. *Trends Pharmacol. Sci.* **2022**, *43* (8), 653–668.
- (33) Laliberte, R. E.; Perregaux, D. G.; Hoth, L. R.; Rosner, P. J.; Jordan, C. K.; Peese, K. M.; Eggler, J. F.; Dombroski, M. A.; Geoghegan, K. F.; Gabel, C. A. Glutathione S-transferase Omega 1–1 Is a target of cytokine release inhibitory drugs and may be responsible for their effect on interleukin-1 $\beta$  posttranslational processing. *J. Biol. Chem.* **2003**, *278* (19), 16567–16578.
- (34) Coll, R. C.; Robertson, A. A. B.; Chae, J. J.; Higgins, S. C.; Muñoz-Planillo, R.; Inserra, M. C.; Vetter, I.; Dungan, L. S.; Monks, B. G.; Stutz, A.; Croker, D. E.; Butler, M. S.; Haneklaus, M.; Sutton, C. E.; Núñez, G.; Latz, E.; Kastner, D. L.; Mills, K. H. G.; Masters, S. L.; Schroder, K.; Cooper, M. A.; O'Neill, L. A. J. A small-molecule inhibitor of the NLRP3 inflammasome for the treatment of inflammatory diseases. *Nat. Med.* **2015**, *21*, 248–255.
- (35) Hochheiser, I. V.; Pilsl, M.; Hagelueken, G.; Moecking, J.; Marleaux, M.; Brinkschulte, R.; Latz, E.; Engel, C.; Geyer, M. Structure of the NLRP3 decamer bound to the cytokine release inhibitor CRID3. *Nature* **2022**, *604*, 184–189.
- (36) Dekker, C.; Mattes, H.; Wright, M.; Boettcher, A.; Hinniger, A.; Hughes, N.; Kapps-Fouthier, S.; Eder, J.; Erbel, P.; Stiefl, N.; Mackay, A.; Farady, C. J. Crystal Structure of NLRP3 NACHT Domain With an Inhibitor Defines Mechanism of Inflammasome Inhibition. *J. Mol. Biol.* **2021**, *433* (24), 167309.
- (37) Dempsey, C.; Rubio Araiz, A.; Bryson, K. J.; Finucane, O.; Larkin, C.; Mills, E. L.; Robertson, A. A. B.; Cooper, M. A.; O'Neill, L. A. J.; Lynch, M. A. Inhibiting the NLRP3 inflammasome with MCC950 promotes non-phlogistic clearance of amyloid- $\beta$  and cognitive function in APP/PS1 mice. *Brain Behav. Immun.* **2017**, *61*, 306–316.
- (38) Gordon, R.; Albornoz, E. A.; Christie, D. C.; Langley, M. R.; Kumar, V.; Mantovani, S.; Robertson, A. A. B.; Butler, M. S.; Rowe, D. B.; O'Neill, L. A.; Kanthasamy, A. G.; Schroder, K.; Cooper, M. A.; Woodruff, T. M. Inflammasome inhibition prevents  $\alpha$ -synuclein pathology and dopaminergic neurodegeneration in mice. *Sci. Transl. Med.* **2018**, *10* (465), eaah4066.
- (39) Ludwig-Portugall, I.; Bartok, E.; Dhana, E.; Evers, B. D. G.; Primiano, M. J.; Hall, J. P.; Franklin, B. S.; Knolle, P. A.; Hornung, V.; Hartmann, G.; Boor, P.; Latz, E.; Kurts, C. An NLRP3-specific inflammasome inhibitor attenuates crystal-induced kidney fibrosis in mice. *Kidney Int.* **2016**, *90* (3), 525–539.
- (40) Perera, A. P.; Fernando, R.; Shinde, T.; Gundamaraju, R.; Southam, B.; Sohal, S. S.; Robertson, A. A. B.; Schroder, K.; Kunde, D.; Eri, R. MCC950, a specific small molecule inhibitor of NLRP3 inflammasome attenuates colonic inflammation in spontaneous colitis mice. *Sci. Rep.* **2018**, *8*, 8618.
- (41) Guo, C.; Fu, R.; Wang, S.; Huang, Y.; Li, X.; Zhou, M.; Zhao, J.; Yang, N. NLRP3 inflammasome activation contributes to the pathogenesis of rheumatoid arthritis. *Clin. Exp. Immunol.* **2018**, *194* (2), 231–243.
- (42) Kim, R. Y.; Pinkerton, J. W.; Essilfie, A. T.; Robertson, A. A. B.; Baines, K. J.; Brown, A. C.; Mayall, J. R.; Ali, M. K.; Starkey, M. R.; Hansbro, N. G.; Hirota, J. A.; Wood, L. G.; Simpson, J. L.; Knight, D. A.; Wark, P. A.; Gibson, P. G.; O'Neill, L. A. J.; Cooper, M. A.; Horvat, J. C.; Hansbro, P. M. Role for NLRP3 Inflammasome-mediated, IL-1 $\beta$ -Dependent Responses in Severe, Steroid-Resistant Asthma. *Am. J. Respir. Crit. Care Med.* **2017**, *196* (3), 283–297.